Effect of the Viscosity and Processing Parameters on the Surface Resistivity of Polypropylene/Multiwalled Carbon Nanotube and Ethylene–Propylene–Diene/Multiwalled Carbon Nanotube Nanocomposites

Kyoung-Tae Min, Gue-Hyun Kim

Division of Energy and Bio Engineering, Dongseo University, Busan 617-716, South Korea

ABSTRACT: In this study, relatively large amounts of polypropylene (PP) and ethylene–propylene–diene (EPDM) were melt-mixed with multiwalled carbon nanotubes (MWCNTs). Although the melt-compounding method has many advantages, the uniform dispersion of carbon nanotubes in the polymer matrix is still the most challenging task. Because the electrical conductivity of composites is strongly influenced by the filler's state of dispersion and the extent of filler breakage during processing, the effects of the viscosity and processing conditions, such as the mixing time, rotor speed, and cooling rate, on the surface resistivity were studied. The PP/MWCNT nanocomposites displayed a high dependence of surface resistivity on the cooling rate, and the EPDM/MWCNT nanocomposites displayed a higher surface resistivity at the same content of MWCNTs and less dependence of surface resistivity on the cooling rate compared with PP/MWCNT nanocomposites. The increased surface resistivity of the EPDM/MWCNT nanocomposites was observed when EPDM with higher viscosity was used to prepare the EPDM/MWCNT nanocomposites. By increasing the rotor speed, lower surface resistivity was obtained in the PP/MWCNT nanocomposites. However, by increasing the rotor speed, a higher surface resistivity was obtained in the EPDM/MWCNT nanocomposites. © 2010 Wiley Periodicals, Inc. J Appl Polym Sci 120: 95–100, 2011

Key words: carbon nanotube; melt; nanocomposites; poly(propylene) (PP); processing

INTRODUCTION

In recent years, the addition of conductive fillers to polymers has been commonly used for electrostatic dissipative purposes. Carbon black is the most widely used filler, but its typical loading is 15–20 wt %; this results in particulate sloughing and, thus, the sacrifice of other desirable properties of the host polymer, such as light weight and toughness. Recently, carbon nanotube (CNT)-based polymer nanocomposites have attracted considerable attention from both fundamental research and application points of view because of the unique combination of mechanical, electrical, and thermal properties of CNTs. The excellent conductivity and very high aspect ratio of CNTs provide polymers with electrical conductivity at low CNT contents. Therefore, CNT-based polymer nanocomposites can be manufactured into electrostatic dissipative parts with smoother surfaces, superior aesthetics, and better mechanical properties.

Although there are many methods for dispersing CNTs into polymers, melt compounding is the most compatible with current industrial practices. This method is also environmentally safe because it is free of the solvents and contaminants that are involved in solution blending and the *in situ* polymerization method. In this aspect, researchers in many studies have recently used the melt-compounding method.[1–32] Because multiwalled carbon nanotubes (MWCNTs) are competitive in cost, most melt-compounding methods have used MWCNTs rather than single-walled CNTs. Although the melt-compounding method has many advantages, the uniform dispersion of CNTs in the polymer matrix is still the most challenging task.

To realize the uniform dispersion of CNTs in the polymer matrix, the effect of the viscosity and processing conditions on the percolation behavior in polymer/MWCNT composites should be well understood. In this study, relatively large amounts of polypropylene (PP; 50 g) and ethylene–propylene–diene (EPDM; 50 g) were melt-mixed with MWCNTs, and the effects of the viscosity, mixing time, rotor speed, and cooling rate on the surface resistivity of the nanocomposites were investigated.

EXPERIMENTAL

Materials and nanocomposite preparation

A commercial PP, H-1500 (Melt index: 12 at 230°C/ 2.1 kg), was provided by LG Chemistry (Seoul, Korea). Three commercial EPDMs, KEP-435 (Mooney viscosity = 33, ethylene content = 56.5 wt %), KEP-240 (Mooney viscosity = 42, ethylene content = 56.5 wt %), and KEP-570 (Mooney viscosity = 53, ethylene content = 70 wt %), were provided by Kumho Polychemical (Seoul, Korea). The MWCNTs were synthesized by thermal chemical vapor deposition (CVD). According to the provider, the typical tube diameter was in the range 10–50 nm with tube lengths of 1–25 μm. The MWCNTs (purity = 95%) were used as received.

PP (or EPDM) and MWCNTs were melt-mixed in a Hakke internal mixer (Waltham, MA) for various times and at various rotor speeds. The mixing temperature was fixed at 175°C. Then, the obtained nanocomposites were compression-molded at 185°C for 10 min.

Testing

The surface resistivity was measured on compression-molded samples (sample dimensions: $110 \times 180 \times 18$ mm^3) with a Worksurface tester ST-3 (SIMCO, Kobe, Japan). Each sample was kept in a desiccator over anhydrous calcium chloride for 48 h before the resistivity measurements. Samples for the resistivity measurements were naturally cooled to room temperature or immediately moved to a cold molder under a minimal pressure. To investigate the dispersion and the length of the MWCNTs in the EPDM/MWCNT nanocomposites, transmission electron microscopy (TEM) images were taken from cryomicrotomed ultrathin sections with an energy filter-transmission electron microscopy EM 912 Omega (Carl zeiss, Oberkochen, Germany). The cross sections of the EPDM/MWCNT nanocomposites were cryogenically microtomed and
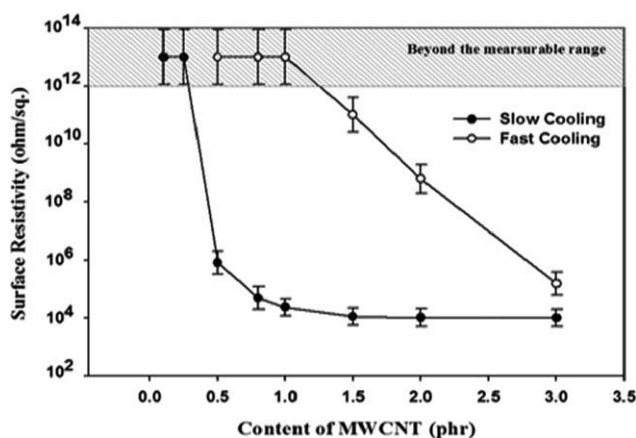

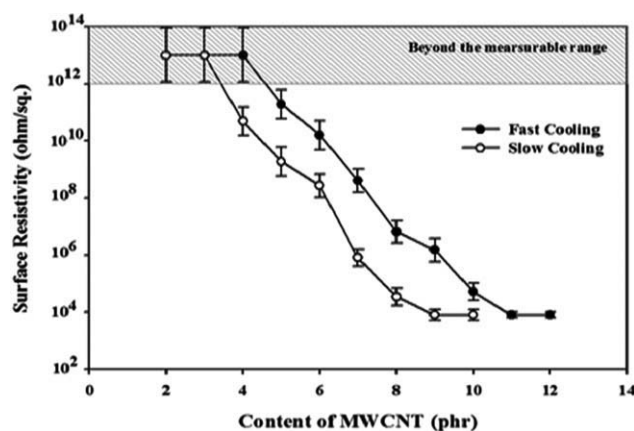**Figure 1** Surface resistivity of the PP/MWCNT nanocomposites with different MWCNT contents.

Figure 2 Surface resistivity of the EPDM/MWCNT nanocomposites with different MWCNT contents.

examined with an energy filter scanning electron microscope JSM-35CF (JEOL, Tokyo, Japan).

RESULTS AND DISCUSSION

For viable electrostatic dissipative applications, the surface resistivity of the polymer/CNT nanocomposites should be in the range 10^5–10^{12} Ω/square (preferably 10^8 Ω/square). The surface resistivity range in our experimental setup was limited to values below 10^{12} Ω/square.

The surface resistivity values of the PP/MWCNT nanocomposites with different MWCNT contents are shown in Figure 1 for slow cooling and fast cooing. In this experiment, PP and MWCNTs were melt-mixed in an intermixer at 60 rpm for 13 min. For fast cooling, the compression-molded samples were immediately moved to a cold molder under minimal pressure. For slow cooling, the compression-molded samples were naturally cooled to room temperature. When slow cooling was applied, a surface resistivity of about 10^4 Ω/square was obtained at 1.5 phr MWCNTs. However, when fast cooling was applied, a surface resistivity of about 10^{11} Ω/square was obtained at 1.5 phr MWCNTs. This was a significant difference, and to the best of our knowledge, this is the first report that recognizes the importance of different cooling rates on the surface resistivity of PP/MWCNT nanocomposites. It is well known that the degree of volume shrinkage depends on the cooling rate. A slow cooling rate leads to larger volume shrinkages. Therefore, the larger volume shrinkages obtained by slow cooling may have led to the smaller distances between neighboring MWCNTs in the PP matrix.

The surface resistivity values of the EPDM/MWCNT nanocomposites with different MWCNT contents are shown in Figure 2 for slow cooling and fast cooing. In this experiment, EPDM and MWCNTs were melt-mixed in an intermixer at 60 rpm for 13 min. EPDM was not crosslinked in this
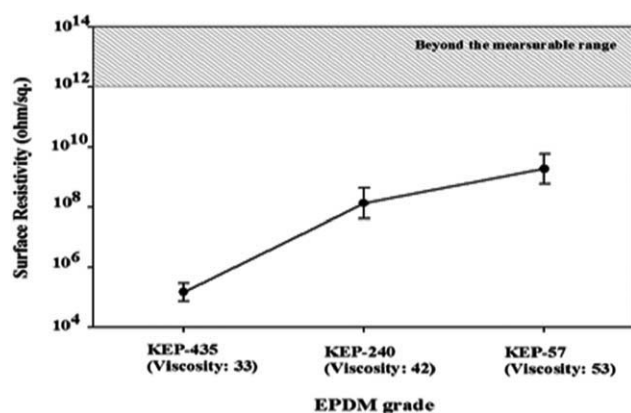
Figure 3 Surface resistivity of the EPDM/MWCNT nanocomposites prepared with different viscosities of EPDM.

experiment. Compared with the PP/MWCNT nanocomposites, the EPDM/MWCNT nanocomposites displayed a higher surface resistivity at the same content of MWCNTs and less dependence of surface resistivity on the cooling rate. The higher surface resistivity of the EPDM/MWCNT nanocomposites compared to that of the PP/EPDM nanocomposites at the same content of MWCNTs could have been due to the higher viscosity of EPDM, which led to a higher shear stress on the MWCNTs during mixing. As a result, the decreased MWCNT length led to an increase in the inter-CNT gap; this resulted in an increase in the surface resistivity. The higher viscosity of the EPDM/MWCNT nanocomposites compared to that of the PP/MWCNT nanocomposites was confirmed by a higher torque value during melt mixing.

To investigate the effect of the viscosity on the surface resistivity of the polymer/MWCNT nanocomposites, EPDM at different viscosities was melt-mixed with 5 phr MWCNTs. Slow cooling was applied for this experiment. Figure 3 shows the increased surface resistivity of the EPDM/MWCNT nanocomposites when EPDM with a higher viscosity was used to prepare the EPDM/MWCNT nanocomposites.

Figure 4 shows TEM micrographs of the MWCNTs in the EPDM matrix with different viscosities. The average length of MWCNTs in the nanocomposite prepared with lower viscosity EPDM [viscosity 33; Fig. 4(a)] was longer than that in the nanocomposites prepared with higher viscosity EPDM [viscosity 53; Fig. 4(b)]. The higher viscosity of EPDM led to a higher shear stress on the MWCNTs during mixing; this resulted in a decrease in the average length of the MWCNTs.

Figure 5 shows the effect of mixing time and rotor speed on the surface resistivity of the PP/MWCNT nanocomposites with a 0.5-phr MWCNT loading. Slow cooling was applied for this experiment. Increasing the rotor speed from 30 to 150 rpm at a mixing time of 6 min led to a decrease in the surface resistivity from greater than 10^{12} to around 10^4 Ω/square. The surface resistivity at mixing times of 13 and 20 min reached 10^4 Ω/square at rotor speeds of 60 and 30 rpm, respectively, and remained at 10^4 Ω/square with further increases in the rotor speed. A short mixing time is preferred for industrial applications. Therefore, for industrial application, a short mixing time and high rotor speed should be chosen
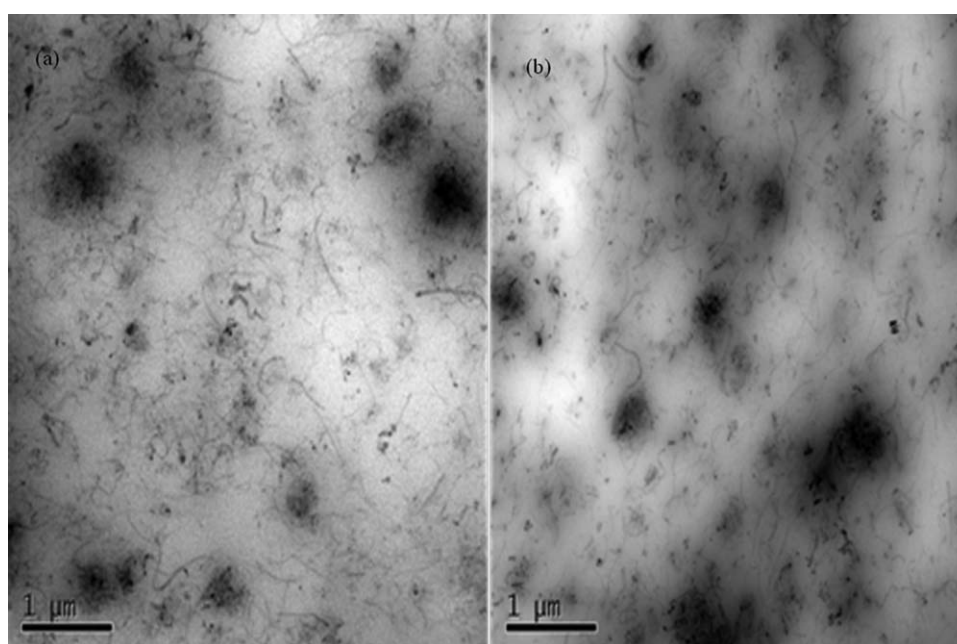

Figure 4 TEM micrographs of MWCNTs in the nanocomposites prepared with (a) lower viscosity EPDM (viscosity = 33) and (b) higher viscosity EPDM (viscosity = 53).
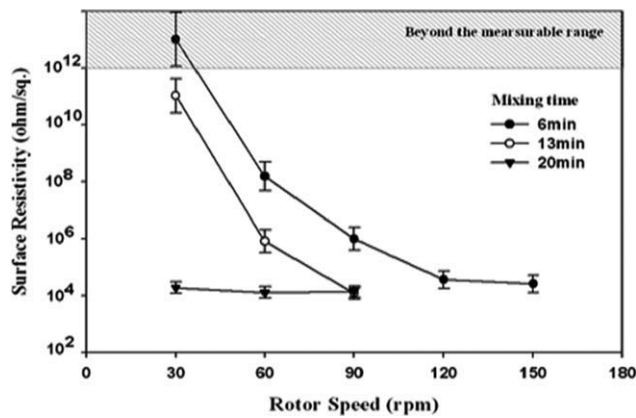
Figure 5 Effect of the mixing time and rotor speed on the surface resistivity of PP/MWCNT nanocomposites with 0.5 phr MWCNTs.

Figure 6 Effect of the mixing time and rotor speed on the surface resistivity of EPDM/MWCNT nanocomposites with 5 phr MWCNTs.

for PP/MWCNT nanocomposites with regard to the surface resistivity.

Figure 6 shows the effect of the mixing time and rotor speed on the surface resistivity of the EPDM/MWCNT nanocomposites with a 5-phr MWCNT loading. Slow cooling was applied for this experiment. At a mixing time of 6 min, the surface resistivity slightly increased with increasing rotor speed.
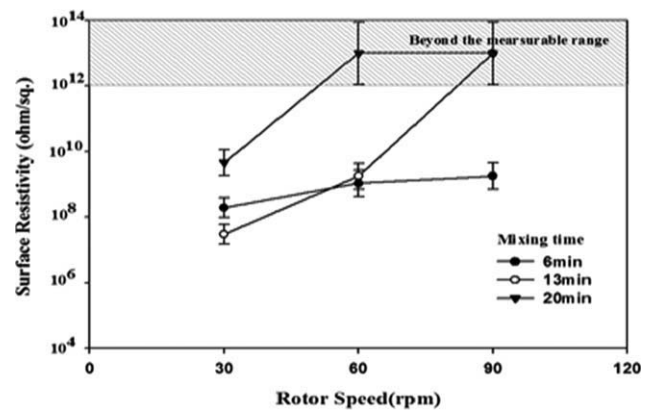
However, at a mixing time of 13 min, increasing the rotor speed from 30 to 90 rpm led to a significant increase in the surface resistivity from around 10^7 to greater than 10^{12} Ω/square.

Figure 7 shows TEM micrographs of the EPDM/MWCNT nanocomposites with a 5-phr MWCNT loading. The MWCNTs in the TEM images were analyzed to obtain the average length with image
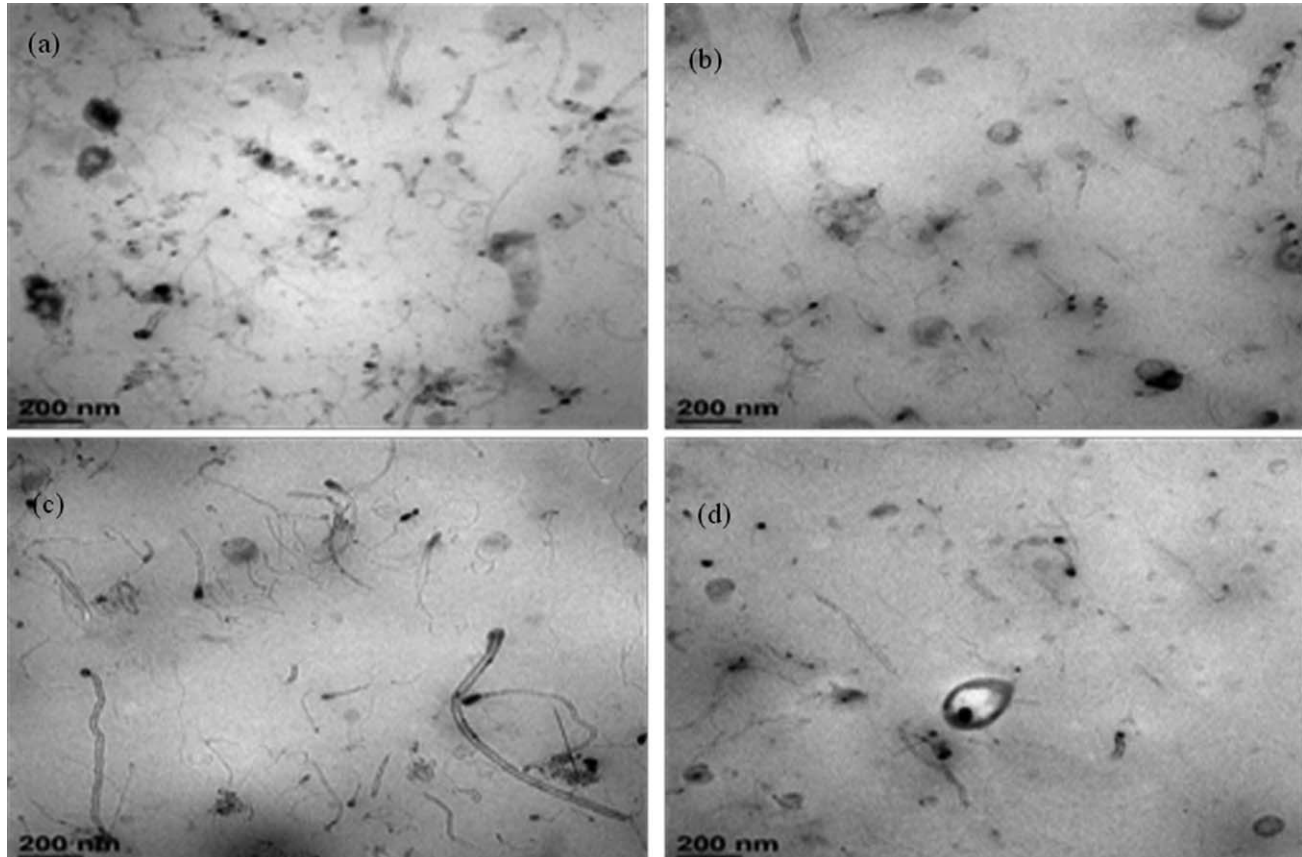

Figure 7 TEM micrographs of MWCNTs in the EPDM/MWCNT nanocomposites prepared with a (a) mixing time of 13 min and rotor speed of 30 rpm, (b) mixing time of 13 min and rotor speed of 90 rpm, (c) mixing time of 20 min and rotor speed of 30 rpm, and (d) mixing time of 20 min and rotor speed of 90 rpm.
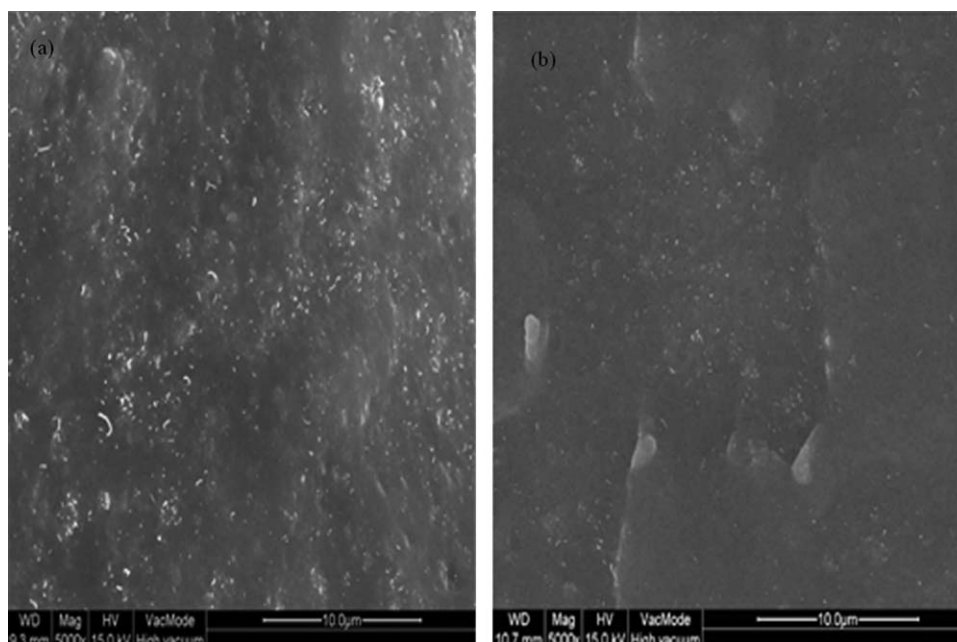
Figure 8 SEM images of the cross sections of EPDM/MWCNT nanocomposites with 5 phr MWCNTs: (a) prepared at a mixing time of 13 min and a rotor speed of 60 rpm and (b) prepared at a mixing time of 13 min and a rotor speed of 90 rpm.

analysis software Kanscope (Mirero, Sungnam, Korea). The average lengths of the MWCNTs shown in Figure 7(a–d) were about 320, 200, 290, and 190 nm, respectively. The dispersion of the MWCNTs in the EPDM matrix improved with increasing mixing time and rotor speed. However, their average length decreased.

In the polymer/MWCNT nanocomposites, an increase in the rotor speed led to an improvement in the dispersion of the MWCNTs in the polymer matrix and a decrease in the MWCNT length. The improvement of dispersion in the MWCNTs resulted in a decrease in the surface resistivity, but a decrease in the MWCNT length led to an increase in the inter-CNT gap; this resulted in an increase in the surface resistivity. Therefore, an increase in the rotor speed at a fixed mixing time produced opposing effects on the surface resistivity.

With increasing rotor speed in the PP/MWCNT nanocomposites (Fig. 5), the effect of the improved dispersion of MWCNTs on the surface resistivity may have overwhelmed the effect of the decreased MWCNT length on the surface resistivity because of the lower viscosity of PP. As a result, a lower surface resistivity was obtained with increasing rotor speed. However, with increasing rotor speed in the EPDM/MWCNT nanocomposites (Fig. 6), the effect of the decreased MWCNT length on the surface resistivity may have overwhelmed the effect of the improved dispersion of MWCNTs because of the higher viscosity of EPDM. This led to a higher shear stress on the MWCNTs during mixing. As a result, a

higher surface resistivity was obtained with increasing rotor speed.

Figure 8 shows SEM images of the cross sections of the EPDM/MWCNT nanocomposites with 5 phr MWCNTs. MWCNTs were easily observed in the nanocomposites prepared at a mixing time of 13 min and a rotor speed of 60 rpm [Fig. 8(a)]. However, it was difficult to observe the MWCNTs in the nanocomposites prepared at a mixing time of 13 min and a rotor speed of 90 rpm [Fig. 8(b)]. This could have been due to the decreased MWCNT length with increased rotor speed.

CONCLUSIONS

In the PP/MWCNT nanocomposites, when slow cooling was applied, a surface resistivity of about 10^4 Ω/square was obtained at 1.5 phr MWCNTs. However, when fast cooling was applied, a surface resistivity of about 10^{11} Ω/square was obtained at 1.5 phr MWCNTs. Compared with the PP/MWCNT nanocomposites, the EPDM/MWCNT nanocomposites displayed a higher surface resistivity at the same content of MWCNTs and less dependence of surface resistivity on the cooling rate.

An increased surface resistivity of the EPDM/MWCNT nanocomposites was observed when EPDM with a higher viscosity was used to prepare the EPDM/MWCNT nanocomposites. According to the TEM results, the average length of MWCNTs in

the nanocomposite prepared with lower viscosity EPDM was longer than that in the nanocomposite prepared with higher viscosity EPDM. A higher viscosity of the polymers led to a higher shear stress on the MWCNTs during mixing. As a result, a decreased MWCNT length led to an increase in the inter-CNT gap. This resulted in an increase in the surface resistivity. In the PP/MWCNT nanocomposites, a lower surface resistivity was obtained when the rotor speed was increased. However, a higher surface resistivity was obtained when the rotor speed was increased in the EPDM/MWCNT nanocomposites. According to the SEM images, the MWCNT length in the EPDM/MWCNT nanocomposites decreased with increased rotor speed.

References

1. Xiao, K. Q.; Zhang, L. C.; Zarudi, I. Compos Sci Technol 2007, 67, 177.
2. McNally, T.; Potschke, P.; Halley, P.; Murphy, M.; Martin, D.; Bell, S. E. J.; Brennan, G. P.; Bein, D.; Lemoine, P.; Quinn, J. P. Polymer 2005, 46, 8222.
3. Kodgire, P. V.; Bhattacharyya, A. R.; Bose, S.; Gupta, N.; Kulkarni, A. R.; Misra, A. Chem Phys Lett 2006, 432, 480.
4. Potschke, P.; Dudkin, S. M.; Alig, I. Polymer 2003, 44, 5023.
5. Potschke, P.; Abdel-Goad, M.; Alig, I.; Dudkin, S.; Lellinger, D. Polymer 2004, 45, 8863.
6. Potschke, P.; Fornes, T. D.; Paul, D. R. Polymer 2002, 43, 3247.
7. Andrews, R.; Jacques, D.; Minot, M.; Rantell, T. Macromol Mater Eng 2002, 287, 395.
8. Grossiord, N.; Loos, J.; Regev, O. O.; Koning, C. E. Chem Mater 2006, 18, 1089.
9. Coleman, J. N.; Khan, U.; Gun'ko, Y. K. Adv Mater 2006, 18, 689.
10. Lisunova, M. O.; Mamunya, Y. E. P.; Lebovka, N. I.; Melezhyk, A. V. Eur Polym J 2007, 43, 949.
11. Zhang, W. D.; Shen, L.; Phang, I. Y.; Liu, T. Macromolecules 2004, 37, 256.
12. Liu, T.; Phang, I. Y.; Shen, L.; Chow, S. I.; Zhang, W. D. Macromolecules 2004, 37, 7214.
13. Alig, I.; Dudkin, S. M.; Jenninger, W.; Marzantowicz, M. Polymer 2006, 47, 1722.
14. Bhattacharyya, A. R.; Sreekumar, T. V.; Liu, T.; Kumar, S.; Ericson, L. M.; Hauge, R. H.; Smalley, R. E. Polymer 2003, 44, 2373.
15. Alig, I.; Lellinger, D.; Dudkin, S. M.; Potschke, P. Polymer 2007, 48, 1020.
16. Li, S. N.; Li, B.; Li, Z. M.; Fu, Q.; Shen, K. Z. Polymer 2006, 47, 4497.
17. Sandler, J. K. W.; Pegel, S.; Cadek, M.; Gojny, F.; Es, M. V.; Lohmar, J.; Blau, W. J.; Schulte, K.; Windle, A. H.; Shaffer, M. S. P. Polymer 2004, 45, 2001.
18. Zhu, D.; Bin, Y.; Matsuo, M. J Polym Sci Part B: Polym Phys 2007, 45, 1037.
19. Valentini, L.; Biagiotti, J.; Kenny, J. M.; Santucci, S. J Appl Polym Sci 2003, 87, 708.
20. Hammel, E.; Tang, X.; Trampert, M.; Schmitt, T.; Mauthner, K.; Eder, A.; Potschke, P. Carbon 2004, 42, 1153.
21. Breuer, O.; Sundararaj, U. Polym Compos 2004, 25, 630.
22. Potschke, P.; Bhattacharyya, A. R.; Janke, A.; Goering, H. Compos Interfaces 2003, 10, 389.
23. Jin, Z.; Pramoda, K. P.; Xu, G. Q.; Goh, S. H. Chem Phys Lett 2001, 337, 43.
24. Jin, Z.; Pramoda, K. P.; Goh, S. H.; Xu, G. Q. Mater Res Bull 2002, 37, 271.
25. Lozano, K.; Barrera, E. V. J Appl Polym Sci 2001, 79, 125.
26. Lozano, K.; Bonilla-Rios, J.; Barrera, E. V. J Appl Polym Sci 2001, 80, 1162.
27. Xiao, K. Q.; Zhang, L. C. J Mater Sci 2005, 40, 6513.
28. Haggenmueller, R.; Gommans, H. H.; Rinzler, A. G.; Fischer, J. E. Chem Phys Lett 2000, 330, 219.
29. Kim, B. S.; Suh, K. S.; Kim, B. Macromol Res 2008, 16, 76.
30. Choi, M.; Lim, B.; Jang, J. Macromol Res 2008, 16, 200.
31. Chen, P.; Kim, H. S.; Jin, H. J. Macromol Res 2009, 17, 207.
32. Han, M. S.; Lee, Y. K.; Kim, W. N.; Lee, H. S.; Joo, J. S.; Park, M.; Lee, H. J.; Park, C. R. Macromol Res 2009, 17, 863.